NEUVIEME COLLOQUE SUR LE TRAITEMENT DU
SIGNAL ET SES APPLICATIONS

NICE du 16 au 20 MAI 1983

NON-PARAMETRIC SIGNAL DETECTION AND IDENTIFICATION OF MODULATION TYPE FOR SIGNALS HIDDEN IN NOISE: AN APPLICATION OF THE NEW THEORY OF CYCLIC SPECTRAL ANALYSIS

William A. Gardner

Signal and Image Processing Laboratory, Department of Electrical and Computer Engineering,
University of California, Davis, CA 95616

RESUME

Cet article considère le problème de l'exploitation de la périodicité cachée dans des données aléatoires afin d'effectuer (i) de la détection de signaux, (ii) de l'estimation de paramètres de signaux (y compris la fréquence et la phase du signal porteur, et la fréquence et la phase de la répétition des impulsions), (iii) de la classification de signaux en fonction du typpe de modulation, y compris des signaux noyés dans le bruit, et (iv) de l'extraction spectrale, qui est l'estimation du spectre d'un signal modulé à partir de mesures sur le signal perturbées par le bruit. Le type de périodicité cachée considérée est une périodicité du second ordre, ce qui inclut tous les types de périodicités pouvant être converties en une composante périodique additive (donnant naissance a des raies spectrales) par une transformation quadratique et invariante dans le temps. La propriété de périodicité du second ordre est caractérisée en termes d'une généralisation du spectre statistique conventionnel, qui est appelée le spectre cyclique. Des généralisations des analyseurs du spectre conventionnel permettant l'analyse du spectre cyclique sont presentées, et il est expliqué comment les utiliser lors de problèmes (i) - (iv). Deux simulations experimentales démontrant l'utilité de l'analyse du spectre cyclique lors de la détection de signaux et lors de l'estimation de fréquences porteuses en modulation d'amplitude avec suppression de porteuse sont presentées. Pour illustrer l'efficacité de l'analyse du spectre cyclique en milieu fortement bruité et en environment perturbé, les données consistent en deux signaux de même puissance, à large bande, modulés en amplitude, avec suppression de porteuse et présentant des recouvrements de spectre significatifs et un rapport signal à bruit pour chacun d'eux: SNR = -6dB.

SUMMARY

ABSTRACT

This paper considers the problem of exploiting hidden periodicity in random data for the purposes of (i) signal detection, (ii) signal parameter estimation (including sinewave carrier frequency and phase, and pulse-repetition frequency and phase), (iii) signal classification according to modulation type, including signals hidden in noise, and (iv) spectral extraction, which is estimation of the spectrum of a modulated signal from noise-corrupted measurements of the signal. The type of hidden periodicity considered is second-order periodicity, which includes all types of periodicity that can be converted into an additive periodic component (which gives rise to spectral lines) with a quadratic, time-invariant transformation. The property of second-order periodicity is characterized in terms of a generalization of the conventional statistical spectrum, which is called the cyclic spectrum. Generalizations of conventional spectrum analyzers that accomplish cyclic spectrum analysis are presented, and it is explained how they can be used for problems (i)-(iv). Two simulation experiments that demonstrate the utility of cyclic spectrum analysis for signal detection and suppressed carrier frequency estimation are presented. To illustrate the capability of cyclic spectrum analysis in a high noise and interference environment, the data consists of two equal-power, broadband, amplitude-modulated, suppressed-carrier signals with significant spectral overlap, and the SNR for each is SNR = -6dB.

NON-PARAMETRIC SIGNAL DETECTION AND IDENTIFICATION OF MODULATION TYPE FOR SIGNALS HIDDEN IN NOISE: AN APPLICATION OF THE NEW THEORY OF CYCLIC SPECTRAL ANALYSIS

William A. Gardner

I. PROBLEM STATEMENT

When random data, x(t), contains hidden periodicity that is not an additive component, and therefore does not give rise to spectral lines, then a common approach to exploiting the periodicity for purposes of detection and estimation (including synchronization) is to transform the data so as to generate spectral lines. The most commonly used devices for accomplishing this are shown in Figures 1 and 2. The device in Figure 1 is frequently used for modulated carrier signals, with $\alpha/2$ ideally equal to the frequency of the suppressed carrier, whereas the device in Figure 2 is often used for modulated pulse signals, with τ ideally equal to half the pulse width, and α ideally equal to the pulse repetition frequency. By tuning α and possibly τ, these devices can be used to detect hidden periodicity and estimate periodicity parameters (frequency and phase). Both devices are sometimes used with signals containing both carrier and pulse modulation. However, these devices do not always perform acceptably. For example for weak signals (such as spread spectrum) in additive noise, they can require an excessive amount of data or respond too slowly (due to narrowness of bandwidth of output BPF).

The major objective of this paper is to put these devices in perspective; i.e., to provide a basis for understanding when and why they work or do not work, and for designing alternative devices, with improved performance. Specifically, we shall consider the most general time-invariant quadratic transformation, which includes as a special case that shown in Figure 3. This device includes the two devices in Figures 1 and 2 as special cases, but this is not the most general time-invariant quadratic device. For example, a parallel connection of a multiplicity of such devices is more general. The most general time-invariant quadratic transformation that can be used to generate spectral lines from hidden periodicity is described in the following definition.

Definition 1. A transformation of a waveform, say x(t), into another waveform, say y(t), is quadratic, time-invariant, and stable if and only if there exists an absolutely integrable* function k(u,v) such that

$$y(t) = \int_{-\infty}^{\infty}\int_{-\infty}^{\infty} k(t-u,t-v)x(u)x(v)dudv ,$$

which is equivalent to

$$y(t) = \int_{-\infty}^{\infty}\int_{-\infty}^{\infty} k(u,v)x(t-u)x(t-v)dudv . \qquad (1)$$

The type of hidden periodicity for which such a device can generate spectral lines is identified in the definitions and theorems presented in Section II.

II. CHARACTERIZATION OF SECOND-ORDER PERIODICITY

Definition 2. A waveform, y(t), contains first-order periodicity with frequency α if and only if the parameter

$$m_y^\alpha \triangleq \lim_{T\to\infty} \frac{1}{T}\int_{-T/2}^{T/2} y(t)e^{-i2\pi\alpha t}dt \neq 0 \qquad (2)$$

exists and is non-zero.

Definition 3. The spectrum of y(t), denoted by $S_y(f)$, is defined by

$$S_y(f) \triangleq \int_{-\infty}^{\infty} R_y(\tau)e^{-i2\pi f\tau}d\tau \qquad (3)$$

*Integrable in each of its arguments

$$R_y(\tau) \triangleq \lim_{T\to\infty} \frac{1}{T}\int_{-T/2}^{T/2} y(t+\tau/2)y(t-\tau/2)dt . \qquad (4)$$

Theorem 1. A waveform, y(t), contains an additive sine-wave component of the form

$$a\cos(2\pi\alpha t+\phi) \qquad (5)$$

if and only if y(t) contains first-order periodicity with frequency α, in which case

$$a = 2|m_y^\alpha|, \qquad \phi = \arg\{m_y^\alpha\} . \qquad (6)$$

Moreover, in this case and only in this case, the spectrum contains the additive component (spectral line)

$$|m_y^\alpha|^2\,[\delta(f-\alpha)+\delta(f+\alpha)] , \qquad (7)$$

for which $\delta(f)$ is the Dirac delta.

Definition 4. A waveform x(t) contains second-order periodicity with frequency α if and only if there exists a stable, time-invariant, quadratic transformation of x(t) into, say, y(t) such that y(t) contains first order periodicity (y(t) exhibits a spectral line) with frequency α.

Theorem 2. A waveform, x(t), contains second-order periodicity with frequency α if and only if the parameter

$$R_x^\alpha(\tau) \triangleq \lim_{T\to\infty} \frac{1}{T}\int_{-T/2}^{T/2} x(t+\tau/2)x(t-\tau/2)e^{-i2\pi\alpha t}dt \neq 0 \qquad (8)$$

exists and is not identically zero, as a function of τ.

We shall call the function $R_x^\alpha(\tau)$ the cyclic autocorrelation, and by analogy with (3), we shall call its Fourier transform, $S_x^\alpha(f)$, the cyclic spectrum

$$S_x^\alpha(f) \triangleq \int_{-\infty}^{\infty} R_x^\alpha(\tau)e^{-i2\pi f\tau}d\tau . \qquad (9)$$

With f fixed, $S_x^\alpha(f)$ is called a cyclic line spectrum since it can be non-zero for only discrete values of α.

An important class of devices that introduce periodicity into an otherwise random waveform is the class of linear periodically time-variant (LPTV) transformations.

Definition 5. An LPTV transformation of z(t) into, say, x(t) is characterized by the superposition integral

$$x(t) = \int_{-\infty}^{\infty} h(t,u)z(u)du \qquad (10)$$

for which $h(t+T_o, u+T_o) = h(t,u)$, where T_o is the (minimal) period.

Example 1: Let w(t) be a random waveform with no second-order periodicity, and let x(t) be the pulse-modulated waveform

$$x(t) = \sum_{n=-\infty}^{\infty} w(nT_c)p(t-nT_c), \qquad p(t) = \begin{cases} 1 & 0 \le t < T_c \\ 0 & \text{otherwise} . \end{cases} \qquad (11)$$

Then x(t) is characterized by (10) with $z = w$ and

$$h(t,u) \triangleq \sum_{n=-\infty}^{\infty} \delta(u-nT_c)p(t-nT_c) . \qquad (12)$$

Furthermore, it can be shown that

$$S_x^\alpha(f) = \begin{cases} \frac{1}{T_o^2} P(f+\alpha/2)P^*(f-\alpha/2) \cdot \\ \sum_{n=-\infty}^{\infty} S_w(f+\alpha/2+n/T_c), & \alpha = k/T_c \\ 0, & \alpha \neq k/T_c \end{cases} \quad (13)$$

where k is an integer and P(f) is the Fourier transform of p(t). The cyclic line spectrum for f = 0 is shown in Figure 4.

Example 2. Let z(t) be a random waveform (possibly containing second-order periodicity), and let x(t) be the carrier-modulated waveform

$$x(t) = z(t)\cos(2\pi f_o t+\phi). \quad (14)$$

Then x(t) is characterized by (10) with

$$h(t,u) = \cos(2\pi f_o t+\phi\ )\delta(t-u). \quad (15)$$

Furthermore, it can be shown that

$$S_x^\alpha(f) = \tfrac{1}{4}[S_z^\alpha(f+f_o) + S_z^\alpha(f-f_o) + S_z^{\alpha+2f_o}(f)e^{-i2\phi} + S_z^{\alpha-2f_o}(f)e^{i2\phi}]. \quad (16)$$

The cyclic line spectrum, for f = center frequency of $S_z(f)$, is shown in Figure 5, for the case in which z(t) contains no second-order periodicity.

Example 3. Let x(t) be the binary phase-shift-keyed signal

$$x(t) = \cos[2\pi f_o t+\phi(t)], \quad \phi(t) = \sum_{n=-\infty}^{\infty} w_n p(t-nT_c) \quad (17)$$

for which $w_n = \pi w(nT_c)$. Then for $w(nT_c) = \pm 1$, we have

$$x(t) = (1/\pi)\phi(t)\cos(2\pi f_o t) ,$$

which is a composite of examples 1 and 2, and therefore $S_x^\alpha(f)$ is given by (13) (with x(t) replaced by z(t) = $(1/\pi)\phi(t)$) and (16). The cyclic line spectrum for f=0 is shown in Figure 6.

Since the LPTV transformation plays such a fundamental role in the introduction of hidden periodicities into otherwise random data, the following theorem is quite important to this subject.

Theorem 3. Let h(t,u) represent an LPTV transformation, (10), with period T_o, and let $\{g_n(\tau)\}$ be the Fourier coefficient functions in the expansion

$$h(t,u) = \sum_{n=-\infty}^{\infty} g_n(t-u)e^{i2\pi nt/T_o} \quad (19)$$

The cyclic spectra for the response x(t) are determined by the cyclic spectra of the excitation according to the formula

$$S_x^\alpha(f) = \sum_{n,m=-\infty}^{\infty} S_z^{\alpha-(n+m)/T_o}(f-[n-m]/2T_o) \cdot G_m(-f+[\alpha/2-m/T_o])G_n(f+[\alpha/2-n/T_o]), \quad (20)$$

for which $G_n(f)$ is the Fourier transform of $g_n(t)$.

Now that we have defined and characterized the type of hidden periodicity that can be converted into spectral lines with a quadratic device, we need to formalize the intuitive notion of the degree (strength) of a periodicity that is hidden in a random waveform.

Neither the cyclic autocorrelation, (8), nor the cyclic spectrum, (9), are directly useful because they are not properly normalized. However, the function

$$C_x^\alpha(f) \triangleq \frac{S_x^\alpha(f)}{[S_x(f-\alpha/2)S_x(f+\alpha/2)]^{\frac{1}{2}}} , \quad (21)$$

which we shall call the autocoherence (or self coherence) function, is indeed properly normalized, and is more generally appropriate as a measure of the degree of second-order periodicity in x(t) because of the properties described in the next theorem.

Theorem 4. (i) The autocoherence function satisfies

$$|C_x^\alpha(f)| \leq 1 \quad (22)$$

for all waveforms x(t). (ii) The autoherence function is invariant to linear time-invariant transformation,

$$C_y^\alpha(f) \equiv C_x^\alpha(f) , \quad (23)$$

for which

$$y(t) = \int_{-\infty}^{\infty} h(t-u)x(u)du , \quad (24)$$

provided that $H(f) \neq 0$, where H(f) is the Fourier transform of h(t).

The following theorem is an important characterization of the autocoherence function.

Theorem 5. Let $z(t) \triangleq x(t)e^{i\pi\alpha t}$ and $y(t) \triangleq x(t)e^{-i\pi\alpha t}$. Then $C_x^\alpha(f)$ is the cross coherence (mutual coherence) of z(t) and y(t),

$$C_x^\alpha(f) \triangleq C_{yz}(f) = \frac{S_{yz}(f)}{[S_y(f)S_z(f)]^{\frac{1}{2}}} , \quad (25)$$

for which $S_{yz}(f)$ is the cross spectrum

$$S_{yz}(f) \triangleq \int_{-\infty}^{\infty} R_{yz}(\tau)e^{-i2\pi f\tau}d\tau \quad (26)$$

$$R_{yz}(\tau) \triangleq \lim_{T\to\infty} \frac{1}{T} \int_{-T/2}^{T/2} y(t+\tau/2)z^*(t-\tau/2)dt. \quad (27)$$

Example 4. Let x(t) be the amplitude/phase-modulated waveform

$$x(t) = a(t)\cos[2\pi f_o t+\phi(t)] = c(t)\cos(2\pi f_o t) - s(t)\sin(2\pi f_o t). \quad (28)$$

It can be shown that

$$R_x^\alpha(\tau) = \tfrac{1}{2}[R_c^\alpha(\tau)+R_s^\alpha(\tau)]\cos(2\pi f_o\tau) + \tfrac{1}{2}[R_{cs}^\alpha(\tau)-R_{sc}^\alpha(\tau)]\sin(2\pi f_o\tau) + \tfrac{1}{4}[R_c^{\alpha+2f_o}(\tau)-R_s^{\alpha+2f_o}(\tau)+R_c^{\alpha-2f_o}(\tau)-R_s^{\alpha-2f_o}(\tau)] - \tfrac{i}{4}[R_{cs}^{\alpha+2f_o}(\tau)+R_{sc}^{\alpha+2f_o}(\tau)-R_{cs}^{\alpha-2f_o}(\tau)-R_{sc}^{\alpha-2f_o}(\tau)]. \quad (29)$$

If c(t) and s(t) contain no second-order periodicity, and $S_c(f) = S_s(f) = 0$ for $|f| > f_o$, then (25) yields

$$|C_x^\alpha(f)| = \frac{[S_c(f)-S_s(f)]^2 + 4[\mathrm{Re}\{S_{cs}(f)\}]^2}{[S_c(f)+S_s(f)]^2 - 4[\mathrm{Im}\{S_{cs}(f)\}]^2} \qquad (30)$$

for $|\alpha| = 2f_o$, and $C_x^\alpha(f) \equiv 0$ for all other α. It follows that $|C_x^\alpha(f)| \equiv 0$ (in which case we shall say that (x(t) is completely incoherent at $\alpha=2f_o$) if and only if

$$S_c(f) \equiv S_s(f), \qquad \mathrm{Re}\{S_{cs}(f)\} \equiv 0 . \qquad (31)$$

At the other extreme, it follows that $|C_x^\alpha(f)| \equiv 1$ (in which case we shall say that x(t) is completely coherent at $\alpha=2f_o$) if and only if

$$|C_{cs}(f)| \equiv 1, \qquad \mathrm{Re}\{S_{cs}(f)\} \neq 0 . \qquad (32)$$

One example of (31) is a single-sideband amplitude-modulated signal for which s(t) is the Hilbert transform of c(t). One example of (32) is a double-sideband amplitude-modulated signal for which s(t) is a scaled version of c(t).

Now that we have(1) defined and characterized the type of periodicity that can be converted into spectral lines with a quadratic device, and (2) defined and characterized the strength of periodicity (degree of coherence), we need to determine specific quadratic devices that are particularly well-suited to generating strong spectral lines. Two alternative implementations of a general purpose quadratic device that can be tuned to produce the strongest possible spectral lines with the minimum amount of data, x(t), (or with the maximum speed of response) are presented in the next section.

III. CYCLIC SPECTRUM ANALYZERS

Since all spectral lines that can be generated from x(t) with a quadratic device are identified by the cyclic line spectrum, then a quadratic device that generates spectral lines with strength $S_x^\alpha(f)$, for any values of α and f, will serve as a general purpose line-generating device. Two alternative implementations of such a device, to be called a cyclic spectrum analyzer, are shown in Figures 7 and 8. In all cases, reliable estimates of $S_x^\alpha(f)$ are obtained only for $\Delta t\Delta f >> 1$, for which Δt is the total integration time (reciprocal bandwidth of output filters) and Δf is the resolution in f (bandwidth of input filters). The resolution in α is $\Delta_\alpha = 1/\Delta t$.

In a sense, the cyclic spectrum analyzer device, with tunable f and α, is equivalent to the device in Figure 2, with tunable τ and α, since it provides an estimate of the cyclic correlation, and the cyclic correlation and cyclic spectrum are a Fourier transform pair, (9). However, analogous to the long established fact that the periodogram is more useful than its inverse Fourier transform, the correlogram, for studying first order periodicity, it turns out that in many cases of practical interest, the cyclic spectrum analyzer is more useful than the cyclic correlation analyzer (Figure 2) for studying second-order periodicity [1]. One important reason for this is that one can collect power at a specific cycle frequency, α, by integrating the cyclic spectrum over appropriate bands of f, and this is accomplished simply by adjusting the center frequencies, and bandwidth, Δf, of the input BPFs in Figure 8, or by adjusting the local oscillator frequencies, $f \pm \alpha/2$, and bandwidth Δf of the input LPFs in Figure 7. Whereas, to collect power with the device in Figure 2, one would need to use a multiplicity of delays, τ. Moreover, for bandpass signals, the individual contributions from different delays, τ, would have to be appropriately weighted with a frequency-shifted sinc function before being summed, because the cyclic correlation is an oscillatory function of τ for bandpass signals. In addition to collecting power at a specific cycle frequency, α, by appropriate choice of f and Δf, larger values of Δf yield more reliable estimates of the cyclic spectrum (integrated over the band of width Δf, centered at f); i.e., degree of randomness of the analyzer output, due to random modulation of the periodicity and to additive noise, is lower when $\Delta t\Delta f$ is larger [1].

IV. DETECTION, ESTIMATION, AND CLASSIFICATION

Since a cyclic spectrum analyzer, in effect, converts hidden periodicity into spectral lines, it can be used together with a threshold device to automatically detect the presence of hidden periodicity. By using the normalization that produces the coherence function, (21), the problem of setting threshold level is greatly simplified.

Since additive noise that contains no periodicity has a cyclic spectrum that is identically zero (for $\alpha \neq 0$), then a cyclic spectrum analyzer can extract the cyclic spectrum of a signal from the corruptive effects of additive noise, n(t). For example, for any arbitrarily broadband amplitude-modulated signal, (14) (with z(t) containing no periodicity), it follows from (16) that the conventional spectrum of the amplitude is

$$S_z(f) = 4S_x^\alpha(f)e^{-i2\phi} \qquad (33)$$

for $\alpha = 2f_o$, and this holds true also when additive noise is present,

$$x(t) = z(t)\cos(2\pi f_o t+\phi) + n(t). \qquad (34)$$

Moreover, the individual spectra for two or more interfering amplitude-modulated signals can be determined provided that their carrier frequencies are different, regardless of the amount of spectral overlap.

Since the cyclic line spectra for different kinds of modulation are distinct (cf. examples 1,2,3), then some signals (hidden in noise) can be classified by measuring their cyclic line spectra.

V. SIMULATION EXPERIMENTS

Experiment 1.

To demonstrate the detection performance of a cyclic spectrum analyzer, we consider a broadband amplitude-modulated suppressed carrier sinewave in additive white Gaussian noise (WGN), (34). The amplitude process, z(t), is WGN that has been bandlimited, by a sliding-rectangular-window smoother (of width 8) to a positive-frequency (first null) bandwidth of 0.125, to yield a signal with power =1/2. Thus, the modulated sinewave has power =1/4. The noise, n(t), is non-bandlimited (i.e., positive frequency bandwidth = 0.5) WGN with power = 1. Thus, the signal-to-noise ratio is SNR = -6dB. The suppressed carrier frequency is f_o = 0.203. A data segment of length Δt = 2048 time-samples was used in the simulation. The spectrum (periodogram = $|X(f)|^2$ = squared magnitude of FFT of data) of the noisy signal, x(t), is shown in Figure 9a. Since there is no additive sinewave component in x(t), there is no spectral line, and the signal cannot be detected from the spectrum. The spectrum of the squared data is shown in Figure 9b. Although the squared data does indeed contain a spectral line, it is masked by the noise, and the signal cannot be detected. (It could be detected

with sufficiently large Δt). The cyclic spectrum of the data is shown in Figure 9c. In order to collect power in the spectral line at $\alpha = 2f_o = 0.406$, Δf was chosen to be quite large, $\Delta f = 0.125 >> \Delta\alpha = 1/\Delta t$ (whereas $\Delta f = 1/\Delta t$ for the spectra in Figures 9a and 9b). Even more power would be collected if Δf were chosen to be larger ($\Delta f = 0.25$ = bandwidth of $S_x^\alpha(f)$ would be optimal). It can be seen from Figure 9c that the signal is easily detected. The cyclic spectrum analyzer in this experiment was implemented by frequency-smoothing (over $[f-\Delta f/2, f+\Delta f/2]$) the conjugate product of frequency-shifted FFTs, $X(f+\alpha/2)X^*(f-\alpha/2)$, as suggested by Theorem 5.

Experiment 2.

To demonstrate the detection performance of a cyclic spectrum analyzer when strong interference as well as strong noise is present, we consider the sum of two broadband amplitude-modulated signals in additive broadband noise. We consider precisely the same model as in Experiment 1, except that two independent signals, with suppressed carrier frequencies of $f_o = 0.203$ and $f_* = 0.328$, are present. Thus, for each of the two signals, SNR = -6dB, and the signal-to-interference ratio is SIR = 0dB. Since the positive-frequency bandwidth of each of these signals is 0.25, which is twice the carrier separation, $f_* - f_o$, then these signals are indistinguishable in the spectrum of $x(t)$, and are, in fact, completely masked by each other and the noise. However, each of the two signals is easily detected with the cyclic spectrum, which is shown in Figure 10. As in experiment 1, $\Delta t = 2048$ and $\Delta f = 0.125$. However, a different implementation of the cyclic spectrum analyzer was used in this experiment. Specifically, a digital implementation of the device shown in Figure 8 was used.

ACKNOWLEDGMENT

The author expresses his gratitude to Mr. William A. Brown for developing the software for the simulations.

REFERENCES

W. A. Gardner, Statistical Spectral Analysis: A Non-Probabilistic Theory, Part II, In preparation for publication.

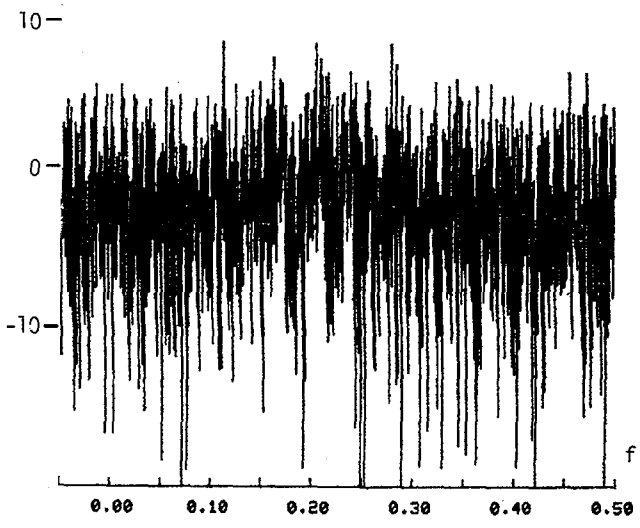

Figure 9a

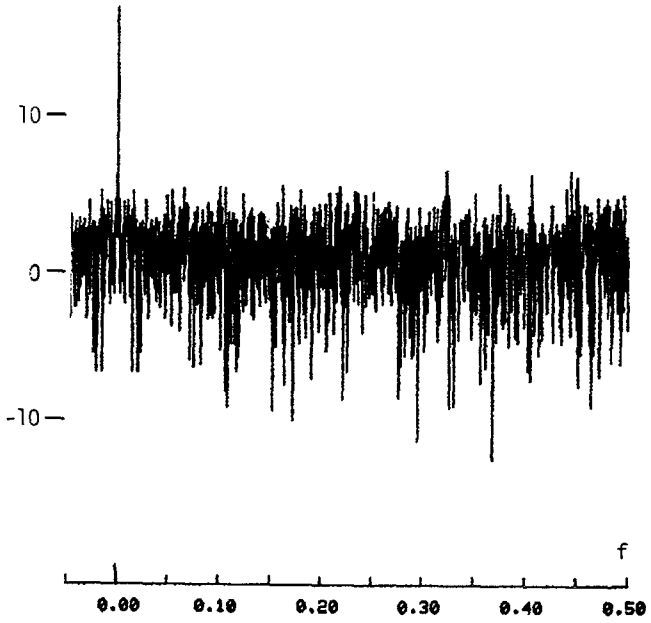

Figure 9b

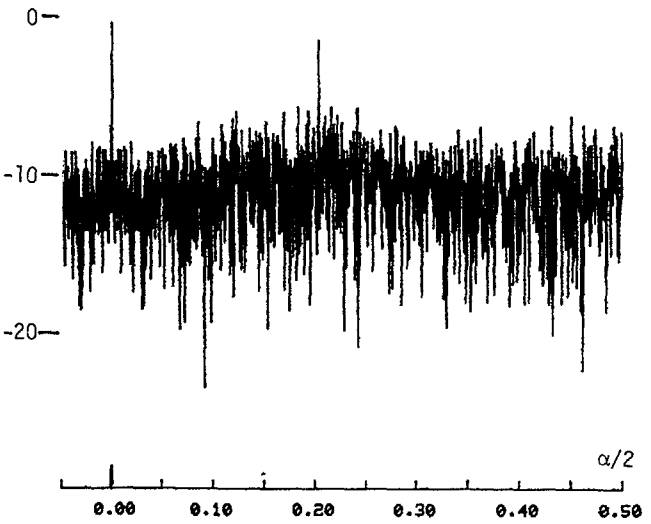

Figure 9c

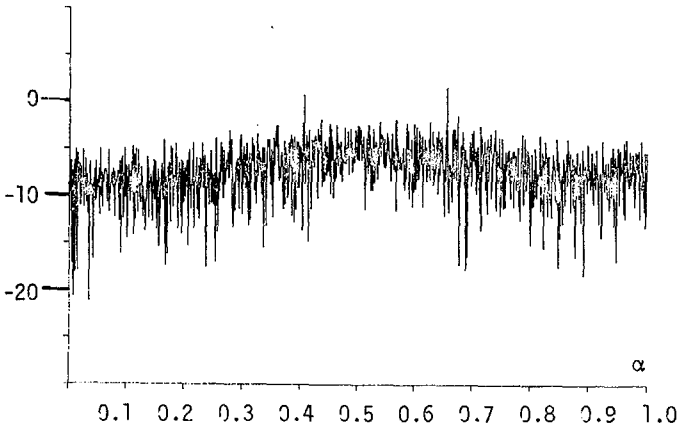

Figure 10

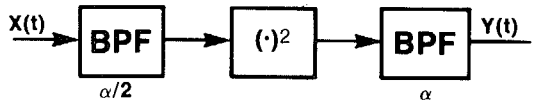

Figure 1

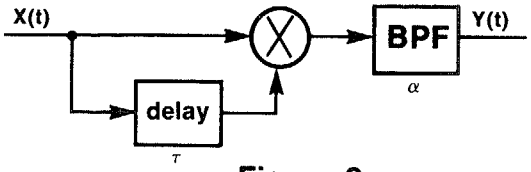

Figure 2

Figure 5

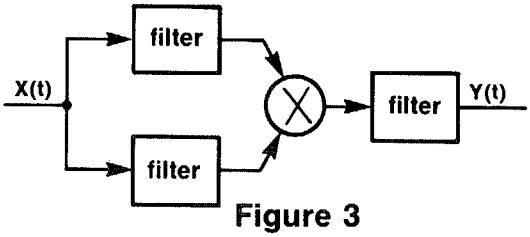

Figure 3

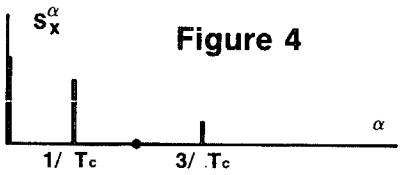

Figure 4

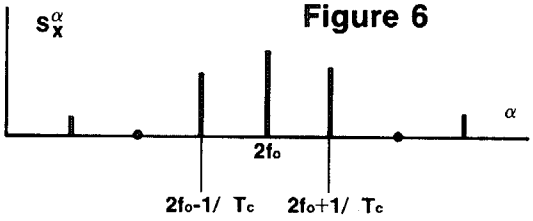

Figure 6

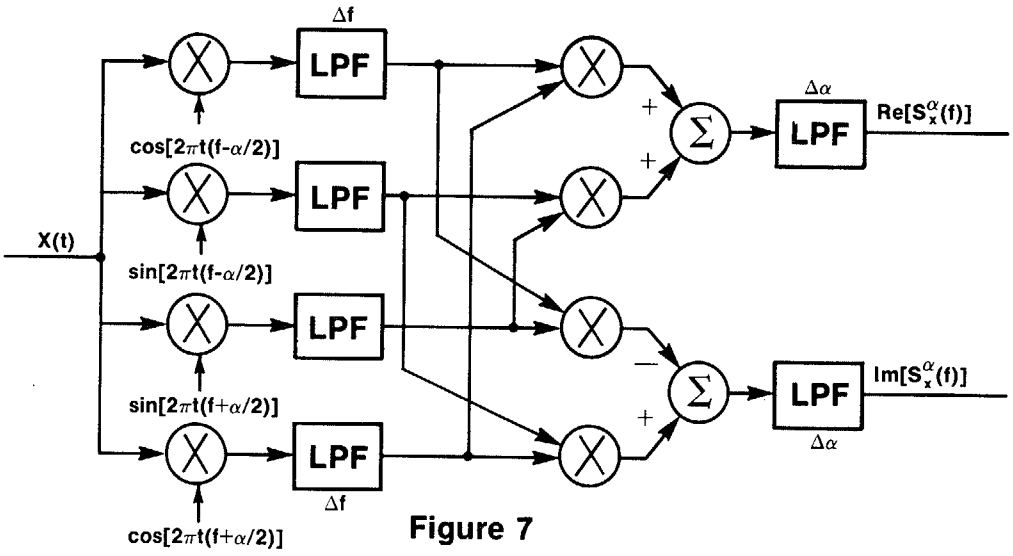

Figure 7

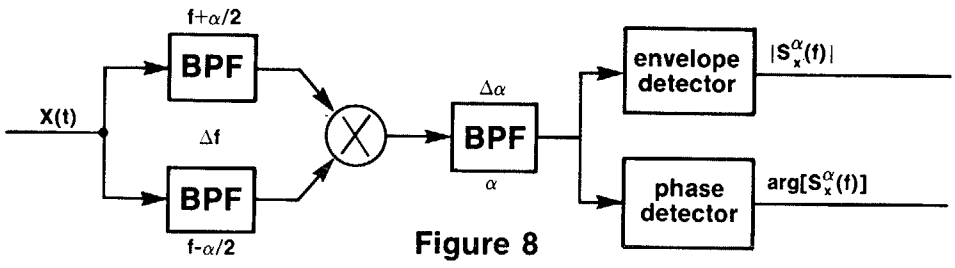

Figure 8